Particle size distribution of organic primary and secondary aerosol constituents in urban, background marine, and forest atmosphere

Ilias G. Kavouras and Euripides G. Stephanou

Environmental Chemical Processes Laboratory, Department of Chemistry, University of Crete, Heraklion, Hellas, Greece

Received 19 December 2000; revised 20 August 2001; accepted 23 August 2001; published 26 April 2002.

[1] Polynuclear aromatic hydrocarbons (PAHs), *n*-alkanes, *n*-alkanals, *n*-alkanols, saturated and unsaturated carboxylic acids, α, ω-dicarboxylic acids, and carbonyl and carboxylic photooxidation products of monoteprenes were determined in particle-sized aerosols of urban (Heraclion, Island of Crete, Greece), background marine (Island of Crete, Greece), and forest (Northern Greece and Portugal) atmospheres. The *n*-alkanes were mostly associated with fine particles in the urban and forest aerosol, and their mass mean aerodynamic diameter (MMAD) calculated over the whole size range (total MMAD) was 0.45 μm and 0.63 μm, respectively. In the background marine aerosol, *n*-alkanes were more evenly distributed, and their MMAD was 2.00 μm, because of physical changes occurring during their long-range transport. Similar observations have been done for PAHs and *n*-alkanals. Conversely, the most biogenic compound class, namely *n*-alkanols, were evenly associated in the urban, background marine, and forest aerosol, between fine and coarse particles, and their corresponding total MMAD was 2.45, 2.69, and 1.67 μm, respectively. The total MMAD of *n*-alkanoic acids was 0.71, 0.62, and 0.91 μm in the urban, background marine, and forest aerosol, respectively. Several compounds associated with photochemical reactions in the atmosphere were detected in urban marine and forests aerosol in the fine and ultrafine fraction, showing the low total MMAD (0.28–0.77 μm) in all aerosol types. *INDEX TERMS:* 0322 Atmospheric Composition and Structure: Constituent sources and sinks; 0365 Atmospheric Composition and Structure: Troposphere—composition and chemistry; 0305 Atmospheric Composition and Structure: Aerosols and particles (0345, 4801)

1. Introduction

[2] The organic fraction of particulate matter is an important and complex matrix of aerosol. It frequently accounts for more than 30% of aerosol mass over continental populated and remote areas [*Andreae et al.*, 1988; *Talbot et al.*, 1992; *Chow et al.*, 1993, 1994]. The total particulate organic carbon, from direct emissions or formed as secondary organic aerosol from atmospheric reactions of volatile organic compounds, has been estimated at $\sim 1-5 \times 10^{12}$ g [*Jaenicke*, 1978; *Hahn*, 1980]. Although organic compounds constitute a large amount of the total dry atmospheric fine-particle mass, their concentration and formation mechanisms are less understood than those of sulfate and nitrate [*Turpin et al.*, 2000]. The ability of organic aerosols to act as cloud condensation nuclei (CCN) seems to be closely related to the chemical properties of their constituents (e.g., polarity, solubility, etc.) and to the physical properties of their particles (e.g., size, surface tension, etc. [*Turpin et al.*, 2000]). A large number of studies focusing on the chemical characterization of the aerosol organic fraction, emitted from different sources, were conducted [*Stephanou*, 1989, 1992; *Stephanou and Stratigakis*, 1993; *Rogge et al.*, 1993a, 1993b, 1993c, 1993d, 1994, 1997a, 1997b, 1998; *Lowenthal et al.*, 1994; *Gogou et al.*, 1996; *Pagano et al.*, 1996; *Kavouras et al.*, 1998a, 1999a; *Simoneit*, 1999]. The mechanisms of the chemical reactions between a variety of unsaturated hydrocarbons and oxidants, and thus their ability to form secondary polar organic aerosol, were investigated in detail [*Atkinson*, 1990; *Atkinson and Arey*, 1998; *Pandis et al.*, 1992]. Furthermore, the chemical coupling of specific polar organic compounds with the formation of new particles formed over forests was established recently in situ [*Kavouras et al.*, 1998b, 1999a, 1999b]. Information concerning the physical and chemical changes of aerosol and its removal from the atmosphere can be found in the literature [*Van Vaeck and Van Cauwenberghe*, 1985; *Sicre et al.*, 1990a; *Aboulkassim and Simoneit*, 1996; *Fernandes et al.*, 1999].

[3] The study of the size distribution of both primary and secondary organic constituents of aerosol is an important factor to assess their role in climate forcing [*Turpin et al.*, 2000], the health hazards involved with particle inhalation [*Pagano et al.*, 1996], and the deposition potential of atmospheric organic carbon. Particle size distributions of *n*-alkanes and polynuclear aromatic hydrocarbons (PAHs) have been mostly studied in the urban environment [*Van Vaeck and Van Cauwenberghe*, 1985; *Aceves and Grimalt*, 1993; *Allen et al.*, 1997; *Kavouras et al.*, 1998a], and in some cases in the marine environment [*Sicre et al.*, 1987, 1990b]. Studies on the size distribution of polar compounds (mainly *n*-alkanoic acids) are very scarce [*Van Vaeck and Van Cauwenberghe*, 1985]. The importance of polar organic aerosol constituents has been recognized because of their role in atmospheric phenomena such as homogeneous nucleation [*Tao and McMurry*, 1989] and impaction of heterogeneous chemistry [*Cruz and Pandis*, 1998]. The effect of polar organic compounds on the formation of clouds was also recently investigated [*Ansari and Pandis*, 2000; *Cruz and Pandis*, 1998; *Russell et al.*, 1994].

[4] In a previous paper we reported a detailed study of the particle size distribution of urban indoor and outdoor aerosol anthropogenic organic compounds such as *n*-alkanes, branched alkanes (environmental tobacco smoke molecular markers), and PAHs [*Kavouras et al.*, 1998a]. Here we report a detailed study on the size distribution of primary and secondary organic constituents of urban, background marine, and forest aerosol collected in different locations of southern Europe. The major goal of the present research was to study the particle size distribution and the atmospheric deposition potential for

0148-0227/02/2000JD000278$09.00

Table 1. Total Suspended Particle (TSP), Extractable Organic Matter (EOM), and Molecular Markers Concentration Ranges[a]

	Urban Aerosol	Background Marine Aerosol	Forest Aerosol
TSP, μg m^{-3}	100.0–192.0	14.0–37.0	1.5–65.0
EOM, μg m^{-3}	12.0–34.0	0.5–8.0	0.1–22.0
n-Alkanes, ng m^{-3}	65.0–320.0	6.5–26.0	10.4–47.0
UCM/NA	8.6–14.0	0.0–6.0	2.2–7.0
PAHs, ng m^{-3}	20.0–60.0	0.1–2.5	0.1–1.2
n-Alkanals, ng m^{-3}	5.5–7.0	1.0–4.0	0.3–2.2
n-Alkanols, ng m^{-3}	17.0–32.0	3.0–17.0	0.1–40.0
n-Alkanoic acids, ng m^{-3}	110.0–200.0	1.0–20.0	14.0–194.0
n-Alkenoic acids, ng m^{-3}	0.0–7.0	0.0–0.6	0.2–103.0
α, ω-Dicarboxylic acids, ng m^{-3}	15.0–47.0	3.0–6.0	0.1–59.0
Pinonaldehyde, ng m^{-3}	ND	ND	0.2–32.0
Nopinone, ng m^{-3}	ND	ND	0.2–13.0
Pinonic acid, ng m^{-3}	ND	ND	0.2–71.0

[a] Other abbreviations are as follows: UCM, unresolved complex mixture concentrations; NA, n-alkane concentration; ND, not detected.

a variety of molecular markers characterizing both primarily emitted and secondarily formed organic aerosols. A series of primary organic aerosol constituents such as aliphatic hydrocarbons, PAHs, *n*-alkanals, *n*-alkanols, *n*-alcanoic acids, and unsaturated carboxylic were identified and studied. Secondary organic aerosol constituents containing dicarboxylic acids and carbonyl and carboxylic compounds produced through the photooxidation of volatile biogenic hydrocarbons were also studied. Taking into consideration the limited particle size resolution of high-volume cascade impactors, we subjected our results to a phenomenological discussion of the aerosol generation processes, as well as of their physical and chemical changes.

2. Experiment

2.1. Sampling of Atmospheric Aerosol

[5] A five-stage (plus backup filter) Sierra Andersen Model 230 Impactor was used mounted on a high-volume pump (GMWL-2000, General Metal Works, Ohio, USA). Aerosol particles were separated into six size fractions on glass-fiber filters, according to their aerodynamic cutoff diameters at 50% efficiency. Namely, the first stage is >7.2 μm, the second stage is 7.2–3.0 μm, the third stage is 3.0–1.5 μm, the fourth stage is 1.5–0.96 μm, the fifth stage is 0.96–0.5 μm, and the backup filter is <0.5 μm at 1.13 m^3 min^{-1} flow rate. After collection, filters were placed in glass tubes and stored in a freezer at −30°C until extraction and analysis.

[6] Six urban size-distributed samples were collected, with a high-volume sampler, in the urban area of the city of Heraclion (150,000 inhabitants) [*Kavouras et al.*, 1998a] during the fall of 1995. Six samples from a background marine site were collected at Environmental Chemical Processes Laboratory sampling station (Finokalia, on the northern coast of Crete, 25°60′E, 35°24′N) from November 1996 to June 1997. The nearest largest city is Heraclion, located 70 km westward of Finokalia. The station is located at the top of a hilly elevation (130 m) facing the sea within the sector of 270° to 90° [*Gogou et al.*, 1996; *Mihalopoulos et al.*, 1997]. Anthropogenic activities are negligible at a distance shorter than 20 km within the above-mentioned sector. Samples were collected for 24 hours under north and south winds which are related with transport from continental Europe and Sahara, respectively [*Mihalopoulos et al.*, 1997]. Nine 12-hour (from 6:00 a.m. to 6:00 p.m. and from 6:00 p.m. to 6:00 a.m.) size-distributed aerosol samples were collected in two forests: (1) an Eucalyptus forest located in Tábua (Portugal) situated 100 km inland from the Atlantic coast [*Kavouras et al.*, 1998b, 1999a] from July to August 1996 and (2) a conifer forest (mainly *Abies Borissi-Regis*) located in Pertouli (1300 m) on the Agrafa mountains in central Greece [*Kavouras et al.*, 1999b] from July to August 1997. The secondary organic aerosol formation versus primary organic aerosol emission and the parameters (e.g., ozone, OH radical, reactive nonmethane hydrocarbons, etc.) influencing these processes were thoroughly described by *Kavouras et al.* [1998b, 1999a, 1999b]. At the above mentioned sampling sites, aerosol samples were also collected, with conventional high-volume samplers, in order to determine the organic aerosol constituents concentration ranges (Table 1) [*Gogou et al.*, 1996; *Kavouras et al.*, 1998a, 1998b, 1999a, 1999b].

2.2. Fractionation, Derivatization, and Identification

[7] A detailed description of the analytical procedure used for extraction, separation, and analysis of the main lipid fractions has been published elsewhere [*Gogou et al.*, 1998]. Briefly, filters were extracted by refluxing methylene chloride for 20 hours. Each organic extract was evaporated using the Kuderna-Danish method, transferred to a 1-mL vial, dried under a gentle stream of nitrogen, and weighted to obtain for each filter the extractable organic matter (EOM). The EOM was then dissolved in a small aliquot of *n*-hexane and applied on the top of a glass column containing specially treated silica gel. Nitrogen pressure was adapted to elute the different compound classes: (1) *n*-hexane for aliphatics, (2) toluene/*n*-hexane for PAHs, (3) *n*-hexane/methylene chloride for carbonyl compounds, (4) ethyl acetate/*n*-hexane for hydroxyl compounds, and (5) a solution of pure formic acid in methanol for carboxylic acids. The individual fractions were spiked with internal standards (1-chlorohexadecane for *n*-alkanes, *n*-alkanals, *n*-alkanol silyl ethers, and for fatty acid methyl esters; hexamethylbenzene for PAH and *n*-hexacosane and long-chain alkenones) for quantitative determinations. Relative response factors, in both gas chromatography-mass spectrometry (GC-MS) and GC-MS in the selected ion monitoring mode, were calculated for 3–10 standard compounds, representing each compound class, of increasing molecular mass. Relative response factors for PAHs were calculated for each single compound individually. Control of procedural blanks has been performed to assess possible contamination. The total blank weight never exceeded 2% of the individual sample extracts (except for the *n*-alkanoic acids, where the maximum contamination represented 10% of the total fraction extract, especially for the homologues C_{14}, C_{16}, and C_{18}). The contaminants were characterized by GC-MS analysis and comparison with standard mixtures. The most frequent contaminants were phthalate esters.

[8] The efficiency of the whole procedure (extraction, fractionation, and derivatization) was very satisfactory. We obtained recoveries (threefold measurements and standard deviation of less than ±3%) of 61.5% up to 98.2% for *n*-alkanes, 60.3% up to 100% for PAHs, 75% for *n*-alkanals, and 88.2% up to 97.7% for *n*-alkanols and 98.3% for fatty acids.

[9] All samples were analyzed on a Finnigan GCQ ion trap gas chromatography-mass spectrometry in the electron impact and occasionally methane-chemical ionization mode [*Kavouras et al.*, 1999a] equipped with a HP-5MS capillary column (30 m × 0.25 mm ID × 0.25 μm film thickness). The temperature ramp for a splitless injection was at 270°C. The chromatographic column

Table 2. Concentration Distribution and Mass Median Aerodynamic Diameter of Particulate Mass and Extractable Organic Matter[a]

Aerodynamic Diameter	Urban Area		Forest Area	
	Particle Mass	Extractable Organic Matter	Particle Mass	Extractable Organic Matter
		Concentration, μgm^{-3}		
>7.2 μm	19.64 ± 3.84	2.04 ± 0.54	4.56 ± 1.98	0.74 ± 0.60
7.2–3.0 μm	23.30 ± 0.22	3.17 ± 0.85	7.81 ± 4.86	1.48 ± 1.53
3.0–1.5 μm	13.75 ± 0.13	1.65 ± 0.43	5.11 ± 2.84	1.09 ± 0.91
1.5–0.96 μm	14.10 ± 2.12	2.10 ± 0.57	6.56 ± 5.20	1.75 ± 1.61
0.96–0.5 μm	79.01 ± 8.93	13.98 ± 1.75	11.38 ± 7.69	3.24 ± 2.24
<0.5 μm	42.28 ± 9.21	11.15 ± 2.96	38.53 ± 26.07	13.07 ± 8.68
		Mass Median Aerodynamic Diameter, μm		
Total	0.81 ± 0.06	0.69 ± 0.05	0.48 ± 0.02	0.41 ± 0.04
Fine	0.67 ± 0.05	0.60 ± 0.04	0.39 ± 0.02	0.36 ± 0.03
Coarse	5.96 ± 0.07	5.59 ± 0.06	5.36 ± 0.02	5.13 ± 0.02

[a] Particle size is defined by Sierra Andersen cascade impactor. Mass median aerodynamic diameters are calculated for the whole range of impactor particle sizes (total) and for fine and coarse particles.

oven temperature was held at 70°C for 2 min. Then, the temperature was increased to 150°C at a rate of 10°C min^{-1}, and then to 290°C at a rate of 5°C min^{-1}. At the end the oven was held at 290°C for 30 min. Mass spectrometer ion source temperature was 200°C, and electron impact ionization potential was 70 eV. The identification was performed by interpretation of mass spectra and by using reference standards for mass spectra comparison (Dr. Ehrenstorfer, Germany).

2.3. Calculations

1. The odd carbon preference indices (CPI) for *n*-alkanes was calculated as follows [*Gogou et al.*, 1996]:

$$\mathrm{CPI} = \Sigma \mathrm{C}_{13} - \mathrm{C}_{35}/\Sigma \mathrm{C}_{12} - \mathrm{C}_{34}.$$

The *n*-Alkanes originating from epicuticular wax of terrestrial plants exhibit high values of CPI (CPI > 1). Conversely, CPI values for *n*-alkanes originating from vehicular emissions and other anthropogenic activities are close to unity (CPI ≈ 1).

2. The wax *n*-alkanes concentration (WNA) was calculated for each *n*-alkane as follows [*Gogou et al.*, 1996]:

$$\mathrm{WNA}\ \mathrm{C}_n = \mathrm{C}_n - 0.5(\mathrm{C}_{n-1} + \mathrm{C}_{n+1}).$$

Negative values of C_n were taken as zero. The percentage of total wax *n*-alkanes to total n-alkanes (%WNA) was calculated as follows:

$$\%\mathrm{WNA} = (\Sigma \mathrm{WNA}\ \mathrm{C}_n/\Sigma \mathrm{NA})100.$$

ΣWNA C_n is the total concentration of wax *n*-alkanes and ΣNA is the total concentration of *n*-alkanes.

3. The size distribution of particles (n^0_{Conc}) can be described as a function of aerodynamic diameter D_a using the Lundgren diagrams as follows [*Van Vaeck and Van Cauwenberghe*, 1985]:

$$n^0_{\mathrm{Conc}} = \frac{dC}{C_T d \log D_a},$$

where C is the concentration (ng m^{-3}) for a given stage, D_a is the aerodynamic diameter (micrometers), and C_T is the total concentration (ng m^{-3}) of a compound.

4. Since cascade impactors classify and collect particles in size ranges, mass mean aerodynamic diameter (MMAD) (particle diameter where one half of the particle mass is smaller and the other half is larger) was stepwise calculated using the following equation for each impactor stage:

$$\left(\int_{D_1}^{D_{\mathrm{MMAD}}} C_i d(D_a) \right) + \sum_{j=1}^{i=1} C_j = \frac{1}{2} C_{\mathrm{total}},$$

where D_{MMAD} is the mass median aerodynamic diameter (micrometers) and D_1 is the lower particle size (micrometers) for *i*-impactor stage; C_i, C_j, and C_{total} are the mass concentrations (ng m^{-3}) for *i*- and *j*-impactor stages and total mass concentration, respectively. If D_{MMAD} was higher than the upper particle size collected by the *i*-impactor stage, the calculation was repeated for the next stage.

3. Results and Discussion

3.1. Size Distribution of Organic Aerosols

[10] Concentration ranges of total suspended particles (TSP) and EOM of the aerosol collected in the urban, background marine, and forest sampling sites are presented in Table 1. In Table 1 the concentration ranges of the organic aerosol constituents, such as *n*-alkanes, PAHs, *n*-alkanals, *n*-alkanols, *n*-alkanoic acids, *n*-alkenoic acids, dicarboxylic acids, and the concentration ratio of unresolved complex mixture of branched hydrocarbons (UCM) and *n*-alkanes investigated in this study are also reported. For the forest aerosol the concentration ranges of pinonaldehyde, nopinone, and pinonic acid, characteristic photo-oxidation products of monoterpenes, are also reported.

[11] Elevated total suspended particulate (TSP) concentration levels (100.0–192.0 μg m^{-3}; Table 1) were determined in the urban environment. The TSP concentration range in Heraclion was similar to that reported in Barcelona [*Aceves and Grimalt*, 1993]. The TSP concentration range in the background marine site (14.0–37.0 μg m^{-3}; Table 1) and the forest sites (1.5–65.0 μg m^{-3}; Table 1) were significantly lower than the corresponding ones of the urban site. TSP concentration in the forest sites exhibited the highest variability (Table 1). This higher variability was also observed for the EOM of the background marine aerosol (0.5–8.0 μg m^{-3}; Table 1) and the forest aerosol (0.1–22.0 μg m^{-3}; Table 1) and to a lesser extent for the urban aerosol (12.0–34.0 μg m^{-3}; Table 1). The impactor stage fractionation (Table 2) shows that urban aerosol can be described by two size-dependent modes. The first mode (fine particles <2.5 μm) corresponds to a mass median aerodynamic diameter (Table 2) of 0.67 μm. This value is higher than the corresponding one determined in the Barcelona aerosol (0.36–0.40 μm [*Aceves and Grimalt*, 1993]). The second mode

Table 3. Organic Molecular Markers Concentration and Diagnostic Parameters Determined in Each Impactor Stage for Urban Aerosol[a]

	Diameter					
	>7.2 μm	7.2–3.0 μm	3.0–1.5 μm	1.5–0.96 μm	0.96–0.5 μm	<0.5 μm
			n-Alkanes			
C_m-C_n; $C_{n,max}$	16–38; 31	18–37; 31	17–37; 31	16–33; 31	19–36; 31	12–34; 27
Concentration, ng m^{-3}	5.0 ± 0.5	5.3 ± 0.9	4.4 ± 0.7	6.2 ± 1.1	13.3 ± 3.4	43.8 ± 9.0
Cumulative concentration, %	100.0	93.6	86.8	81.2	73.2	56.2
CPI	1.7 ± 0.3	1.8 ± 0.4	1.6 ± 0.2	1.6 ± 0.1	1.5 ± 0.5	1.2 ± 0.3
UCM	53.0 ± 15.1	60.7 ± 12.2	43.7 ± 9.8	74.5 ± 34.9	173.1 ± 68.0	692.4 ± 94.4
UCM/NA	12.7 ± 2.6	10.8 ± 4.3	8.2 ± 2.2	11.9 ± 3.2	13.0 ± 4.0	15.8 ± 4.4
Percent WNA	29.5 ± 4.1	29.4 ± 4.9	22.4 ± 3.1	23.8 ± 3.6	23.8 ± 5.2	17.8 ± 3.3
			PAHs			
Concentration, pg m^{-3}	60 ± 20	60 ± 10	140 ± 40	300 ± 90	540 ± 120	2,540 ± 330
Cumulative concentration, %	100.0	98.4	96.7	92.9	84.6	69.8
CPAHs/TPAHs	0.46 ± 0.12	0.61 ± 0.11	0.58 ± 0.08	0.82 ± 0.13	0.73 ± 0.09	0.67 ± 0.10
TPhs/TPAHs	0.34 ± 0.09	0.14 ± 0.02	0.20 ± 0.04	0.05 ± 0.02	0.10 ± 0.04	0.07 ± 0.03
			n-Alkanals			
C_m-C_n; $C_{n,max}$	ND	9	9	17–19; 17	9; 17	16–23; 22
Concentration, pg m^{-3}	...	40 ± 10	70 ± 20	100 ± 50	60 ± 20	350 ± 70
Cumulative concentration, %	100.0	100.0	93.5	82.3	66.1	56.5
CPI	...	...	...	...	...	2.4 ± 1.3
			n-Alkanols			
C_m-C_n; $C_{n,max}$	14–32; 28	14–32; 28	14–30; 28	14–28; 26	14–30; 30	14–32; 28
Concentration, ng m^{-3}	2.3 ± 0.5	2.8 ± 0.3	2.0 ± 0.2	1.0 ± 0.2	1.4 ± 0.1	2.5 ± 0.3
Cumulative concentration, %	100.0	80.8	57.5	40.8	32.5	20.8
CPI	3.1 ± 1.0	5.1 ± 0.6	5.0 ± 1.0	6.5 ± 1.0	5.1 ± 0.8	3.1 ± 0.3
			n-Alkanoic Acids			
C_m-C_n; $C_{n,max}$	14–21; 16	14–18; 16	14–18; 16	12–24; 16	8–28; 16	12–28; 18
Concentration, ng m^{-3}	0.9 ± 0.1	0.2 ± 0.1	0.8 ± 0.1	74.4 ± 4.0	470.9 ± 35.0	110.4 ± 9.9
Cumulative concentration, %	100.0	99.9	99.8	99.7	88.4	16.8
CPI	13.7 ± 1.1	15.6 ± 1.6	18.7 ± 2.8	18.6 ± 3.9	19.1 ± 2.5	10.6 ± 1.0
			n-Alkenoic Acids			
C_m-C_n; $C_{n,max}$	16:1,18:1	16:1,18:1	16:1,18:1	16:1,18:1	16:1,18:1	16:1,18:1
Concentration, ng m^{-3}	0.2 ± 0.1	0.6 ± 0.2	1.0 ± 0.3	6.2 ± 0.6	4.3 ± 3.0	5.5 ± 1.6
Cumulative concentration, %	100.0	98.9	95.5	89.9	55.1	30.9
			α, ω-*Dicarboxylic Acids*			
C_m-C_n; $C_{n,max}$	ND	ND	ND	9	6–10; 9	6–15; 9
Concentration, ng m^{-3}	...	...	...	1.7 ± 0.5	4.7 ± 1.1	17.6 ± 4.6
Cumulative concentration, %	...	...	...	100	92.9	73.3

[a] Abbreviations are as follows: C_n-C_m, homologue concentration ranges; $C_{n,max}$, homologues with the maximum concentration for molecular markers; CPI, carbon preference index; UCM, unresolved complex mixture; NA, total *n*-alkanes; WNA, leaf wax *n*-alkanes; PAHs, polynuclear aromatic hydrocarbons; CPAHs, combustion-derived PAHs; TPAHs, total PAHs concentration; TPhs, total phenanthrenes.

(coarse particles >2.5 μm), for the urban (city of Heraclion) aerosol, corresponds to a MMAD of 5.96 μm. This value is in the same order of magnitude as that determined in Barcelona (4.6–6.0 μm). The smaller particle stages (<1.5 μm) in urban aerosol contain most of the TSP mass (~71%, calculated from Table 2). The EOM was also described by two size-dependent modes in the urban aerosol. EOM was distributed between fine particles with a MMAD of 0.60 μm (Table 2) and coarse particles with a MMAD of 5.59 μm (Table 2). In the urban aerosol the smaller particle stages (<1.5 μm) contained most of the EOM mass (~80% calculated from Table 2). MMDA calculated for the whole range of impactor sizes is 0.81 μm (Table 2) for particulate matter (PM) and 0.69 μm (Table 2) for EOM. Forest aerosol differed from the urban one when we consider the above parameters. MMDA calculated for total particle size range for forest aerosol was 0.48 μm (Table 2) for PM and 0.41 μm (Table 2) for EOM. For forest aerosol the impactor stage fractionation showed that fine particles (<2.5 μm) correspond to a MMAD of 0.39 μm for PM and 0.36 μm for EOM (Table 2). These values are considerably lower than the corresponding ones determined in urban aerosol (Table 2). Coarse particles (>2.5 μm) for forest aerosol correspond to a MMAD of 5.36 μm for PM and 5.13 μm for EOM. The smaller particle stages (<1.5 μm) in the forest aerosol contained most of the PM (~76%, calculated from Table 2) and EOM (81%, calculated from Table 2) mass. The concentrations of particulate matter (4.56–7.81 μg m^{-3}; Table 2) and extractable organic carbon (0.74–1.48 μg m^{-3}; Table 2) associated with large particles (D_a > 1.5) were lower than those measured for smaller particles (D_a < 1.5) (particulate matter is 6.56–38.53 μg m^{-3} and organic carbon is 1.75–13.07 μg m^{-3}; Table 2). These results suggest that the increase of aerosol mass is due to the higher contribution of organic compounds. These compounds can be associated with either direct emissions of lipids from the trees or condensation of low-vapor organic gases formed through the photooxidation of unsaturated hydrocarbons or both [*Kavouras et al.*, 1998b, 1999a, 1990b]. The MMAD of an organic compound is found at a significantly smaller particle size than for the total aerosol if a condensation mechanism prevails. This should be the case in the forest aerosol since the gas-particle conversion enriches the aerosol fraction in the smaller particle size range [*Kavouras et al.*, 1999b].

[12] Organic aerosol molecular markers such as aliphatic hydrocarbons, unresolved complex mixture (UCM) of branched hydro-

Table 4. Organic Molecular Marker Concentration and Diagnostic Parameters Determined in Each Impactor Stage for Marine Background Aerosol[a]

	Diameter					
	>7.2 μm	7.2–3.0 μm	3.0–1.5 μm	1.5–0.96 μm	0.96–0.5 μm	<0.5 μm
				n-Alkanes		
C_m-C_n; $C_{n,max}$	17–39; 29	17–39; 29	17–39; 31	17–39; 31	17–39; 31	17–39; 31
Concentration, ng m^{-3}	0.5 ± 0.1	1.9 ± 0.2	0.8 ± 0.1	0.7 ± 0.1	0.9 ± 0.2	1.0 ± 0.1
Cumulative concentration, %	100.0	91.9	59.2	45.3	32.3	17.2
CPI	2.3 ± 0.6	1.7 ± 0.2	1.6 ± 0.2	1.9 ± 0.1	1.7 ± 0.2	1.8 ± 0.2
UCM	0.8 ± 0.1	3.5 ± 1.0	1.1 ± 0.2	1.5 ± 0.2	1.7 ± 0.6	2.0 ± 0.2
UCM/NA	1.2 ± 0.2	1.9 ± 0.6	1.5 ± 0.7	2.0 ± 0.4	2.0 ± 0.9	2.0 ± 0.1
Percent WNA	41.3 ± 10.2	26.8 ± 6.3	25.8 ± 8.2	32.8 ± 12.2	21.2 ± 7.0	30.8 ± 2.7
				PAHs		
Concentration, pg m^{-3}	30 ± 10	20 ± 10	30 ± 10	50 ± 20	60 ± 20	120 ± 40
Cumulative concentration, %	100.0	90.4	83.9	74.2	58.1	38.7
CPAHs/TPAHs	...	...	...	0.42 ± 0.04	0.52 ± 0.07	0.63 ± 0.09
TPHs/TPAHs	...	...	...	0.01 ± 0.01	0.09 ± 0.02	0.08 ± 0.01
				n-Alkanals		
C_m-C_n; $C_{n,max}$	12–29; 26	13–29; 26	12–29; 26	12–29; 28	12–29; 28	12–29; 28
Concentration, ng m^{-3}	0.2 ± 0.0	0.3 ± 0.1	0.9 ± 0.2	1.4 ± 0.2	0.8 ± 0.2	1.0 ± 0.2
Cumulative concentration, %	100.0	96.6	90.6	70.3	39.3	21.1
CPI	2.0 ± 0.5	3.4 ± 0.1	5.0 ± 1.1	8.1 ± 2.1	3.5 ± 1.2	6.2 ± 2.2
				n-Alkanols		
C_m-C_n; $C_{n,max}$	12–30; 28	14–30; 28	12–30; 28	12–26; 24	12–28; 28	12–29; 28
Concentration, ng m^{-3}	0.1 ± 0.1	0.7 ± 0.2	0.4 ± 0.2	0.2 ± 0.1	0.2 ± 0.1	0.2 ± 0.1
Cumulative concentration, %	100.0	94.5	55.2	30.6	21.9	9.3
CPI	2.9 ± 0.5	4.4 ± 1.1	4.9 ± 0.8	11.1 ± 1.1	4.7 ± 1.1	5.1 ± 0.5
				n-Alkanoic Acids		
C_m-C_n; $C_{n,max}$	14–21; 16	14–20; 16	12–20; 16	12–24; 16	10–26; 16	9–25; 16
Concentration, ng m^{-3}	1.7 ± 0.7	4.3 ± 1.1	4.2 ± 0.6	6.7 ± 1.15	13.6 ± 3.3	23.5 ± 4.4
Cumulative concentration, %	100.0	96.9	88.9	81.1	68.7	43.6
CPI	11.1 ± 1.1	12.3 ± 5.4	14.4 ± 2.2	24.5 ± 5.5	20.9 ± 5.1	19.0 ± 6.2
				n-Alkenoic Acids		
C_m-C_n; $C_{n,max}$	16–20	16–20	16–20	16–20	16–20	16–20
Concentration, ng m^{-3}	0.4 ± 0.2	0.3 ± 0.1	1.0 ± 0.6	0.4 ± 0.1	0.5 ± 0.1	0.6 ± 0.1
Cumulative concentration, %	100.0	86.7	76.4	47.0	33.8	19.1
				α, ω-*Dicarboxylic Acids*		
C_m-C_n; $C_{n,max}$	ND	ND	ND	9	8–10; 9	7–15; 9
Concentration, ng m^{-3}	...	...	...	1.1 ± 0.1	0.8 ± 0.3	1.0 ± 0.4
Cumulative concentration, %	...	...	...	100.0	61.2	34.2

[a] For abbreviations, see Table 3.

carbons, PAHs, *n*-alkanals, *n*-alkanols, *n*-alkanoic, and *n*-alkenoic and dicarboxylic acids were identified in the samples of the studied sampling sites (Table 1). The influence of air masses origin [*Mihalopoulos et al.*, 1997] on TSP, EOM, and the above molecular markers has been reported elsewhere [*Gogou et al.*, 1996]. The *n*-Alkanes dominated the aliphatic aerosol fraction of all samples. The study of these parameters confirmed a stronger input of biogenic *n*-alkanes in background marine and forest aerosol than in the urban samples. Lower UCM/*n*-alkanes concentration ratios were observed (UCM/NA, Table 1) in the marine (0.0–6.0; Table 1) and forest (2.2–7.0; Table 1) samples than in the urban ones (8.6–14.0; Table 1), thus indicating a lower contribution of petroleum hydrocarbons. In the forest samples the relative homologue distribution was correlated with this obtained from forest trees epicuticular wax extract [*Kavouras et al.*, 1999a]. The *n*-Alkanals, *n*-alkanols, and carboxylic acids were also identified in all samples (Table 1). In the forest aerosol these lipids originated mainly from epicuticular wax of forest trees [*Kavouras et al.*, 1999b]. In urban and background marine samples the above lipids had a rather mixed origin [*Gogou et al.*, 1996]. In urban samples, *n*-alkanals homologues distribution demonstrated a mixed origin from microbial sources and *n*-alkanes oxidation [*Stephanou*, 1989]. Conversely, in background marine samples the *n*-alkanal homologues distribution was very similar to the corresponding pattern of *n*-alkanols. The similarity of the homologue distribution between *n*-alkanols and *n*-alkanals indicated a close relationship and thus a common origin (terrestrial higher plant wax) of these two compound classes [*Gogou et al.*, 1996]. The concentrations of *n*-alkanals in the urban area (5.5–7.0 ng m^{-3}; Table 1) were higher than those measured in the background marine site (1.0–4.0 ng m^{-3}; Table 1) and the forest areas (0.3–2.2 ng m^{-3}; Table 1). The most abundant compound class determined among the neutral oxygenated lipids was that of *n*-alkanols (17.0–32.0 ng m^{-3} for urban, 3.0–17.0 ng m^{-3} for marine, and 0.1–40.0 ng m^{-3} for forest aerosol; Table 1). Carboxylic acids were by far the most abundant compound class detected in all collected samples (Table 1). We detected four different groups of carboxylic acids, namely *n*-alkanoic, *n*-alkenoic, dicarboxylic acids [*Stephanou and Stratigakis*, 1993; *Gogou et al.*, 1996], and a series of carboxylic acids considered as photooxidation products of monoterpenes [*Kavouras et al.*, 1998a, 1999a, 1999b]. The latter were detected only in the forest atmosphere (0.2–71.0 ng m^{-3}). The *n*-Alkanoic acids varied from 110.0 to 200.0 ng m^{-3} in the urban, 1.0 to 20.0 ng m^{-3} in the marine, and 14.0 to 194.0 ng m^{-3} in the forest atmosphere (Table 1). The *n*-Alkenoic acids, because of their

Table 5. Organic Molecular Marker Concentration and Diagnostic Parameters Determined in Each Impactor Stage for Forest Aerosol[a]

	Diameter					
	>7.2 μm	7.2–3.0 μm	3.0–1.5 μm	1.5–0.96 μm	0.96–0.5 μm	<0.5 μm
			n-Alkanes			
C_m-C_n; $C_{n,max}$	17–41; 29	17–45; 29	17–45; 31	17–45; 29	17–45; 29	17–45; 29
Concentration, ng m^{-3}	3.5 ± 1.0	3.3 ± 0.4	1.2 ± 0.2	5.9 ± 0.9	11.9 ± 1.3	19.1 ± 4.3
Cumulative concentration, %	100.0	92.0	84.7	82.1	69.0	42.5
CPI	2.5 ± 0.8	2.4 ± 0.9	2.4 ± 0.2	2.2 ± 0.9	2.2 ± 0.9	2.6 ± 1.0
UCM	76.6 ± 15.5	42.3 ± 15.5	17.2 ± 7.0	50.9 ± 14.8	274.6 ± 54.8	1270.1 ± 154.1
UCM/NA	22.7 ± 5.	21.6 ± 3.3	12.7 ± 3.7	8.5 ± 4.2	18.1 ± 8.6	99.7 ± 4.6
Percent WNA	46.0 ± 10.2	43.8 ± 11.3	57.3 ± 10.7	37.5 ± 7.3	37.4 ± 9.2	37.5 ± 8.6
			PAHs			
Concentration, pg m^{-3}	10 ± 10	10 ± 10	10 ± 10	10 ± 10	40 ± 20	60 ± 20
Cumulative concentration, %	100.0	92.8	85.7	78.6	71.5	42.9
CPAHs/TPAHs	...	0.27 ± 0.09	0.76 ± 0.10	0.89 ± 0.14	0.76 ± 0.38	0.09 ± 0.08
TPHs/TPAHs	...	0.24 ± 0.12	...	...	0.08 ± 0.02	0.84 ± 0.42
			n-Alkanals			
Concentration, ng m^{-3}	...	...	...	...	...	...
			n-Alkanols			
C_m-C_n; $C_{n,max}$	12–28; 20,26	12–26; 20,26	16–26; 20,26	18–26; 20,26	12–26; 20,26	12–26; 20,26
Concentration, ng m^{-3}	2.1 ± 0.9	1.4 ± 1.0	2.0 ± 0.8	1.9 ± 0.7	2.3 ± 1.1	2.2 ± 0.9
Cumulative concentration, %	100.0	82.3	70.2	53.6	38.0	18.5
CPI	30.9	NC	NC	NC	NC	NC
			n-Alkanoic Acids			
C_m-C_n; $C_{n,max}$	12–30; 16	12–30; 16	12–30; 16	12–30; 16	12–30; 16	12–28; 16
Concentration, ng m^{-3}	9.9 ± 2.2	25.5 ± 4.5	44.0 ± 10.0	49.9 ± 8.3	39.1 ± 8.2	98.1 ± 18.1
Cumulative concentration, %	100.0	96.3	86.7	70.2	51.5	36.8
CPI	6.7 ± 3.2	6.1 ±.2.6	5.1 ± 0.6	5.4 ± 1.3	5.0 ± 0.5	8.8 ± 4.0
			Alkenoic Acids			
C_m-C_n; $C_{n,max}$	15–18	15–18	15–18	15–18	15–18	15–18
Cumulative concentration, %	3.55 ± 1.10	6.45 ± 0.98	5.55 ± 2.22	6.14 ± 1.64	6.66 ± 2.22	8.99 ± 3.84
Concentration, %	9.5	17.27	14.9	16.4	17.8	24.1
			α, ω-*Dicarboxylic Acids*			
C_m-C_n; $C_{n,max}$	8–11; 9	8–11; 9	8–11; 9	8–11; 9	6–11; 9	6–11; 9
Cumulative Concentration, %	0.2 ± 0.1	0.2 ± 0.0	0.8 ± 0.1	0.3 ± 0.0	0.3 ± 0.1	4.4 ± 1.6
Concentration, %	100.0	97.3	94.3	81.8	77.5	72.9
			Terpenoid Compounds, ng m-3			
Nopinone	ND	ND	ND	ND	0.2 ± 0.1	0.2 ± 0.1
Cumulative Concentration, %	...	...	...	...	100.0	55.6
Pinonaldehyde	ND	ND	ND	0.3 ± 0.00	0.2 ± 0.2	2.0 ± 1.1
Cumulative Concentration, %	...	...	...	100.0	88.9	79.0
Pinonic acid	ND	ND	ND	0.4 ± 0.2	2.2 ± 1.0	8.5 ± 4.3
Cumulative Concentration, %	...	...	...	100.0	96.0	75.9

[a] For abbreviations, see Table 3; NC is not calculated.

higher reactivity [*Stephanou and Stratigakis*, 1993], were determined in lower concentration in the urban and marine atmosphere (Table 1). In the forest atmosphere, because of their continuous emission [*Kavouras et al.*, 1999a], the concentration was higher (up to 103 ng m^{-3}; Table 1). The organic aerosol molecular markers described above were also identified in each impactor stage of the samples collected at the sampling sites (Tables 3–5).

[13] The analysis of the *n*-alkane homologues allowed the determination for each impactor stage of their relative distribution ($C_m - C_n$), homologue with the maximum concentration ($C_{n,\,max}$), the UCM concentration, the CPI, and the percentage of leaf wax *n*-alkane content (%WNA).

[14] In the urban aerosol the bulk (~81%, calculated from Table 3) of *n*-alkane concentration was determined in particles with diameters <1.5 μm. The CPI of *n*-alkanes in all impactor stages (Table 3) exhibited a mixed origin (petroleum residues and higher plant wax) of *n*-alkanes. The *n*-alkanes associated with particles <0.5 μm demonstrated the lowest CPI values (1.2 ± 0.3; Table 3). UCM was mostly associated (~86%, calculated from Table 3) with particles <1.5 μm. Conversely, WNA showed a preference to particles >1.5 μm (Table 3). In the background marine aerosol a clear trend for the *n*-alkane size distribution was not determined. The *n*-alkane concentration was more evenly distributed between particle sizes (Table 4). The same observation can be made for CPI, UCM, and %WNA (Table 4). These facts probably reflect the physical changes (e.g., particle size changes and wet and dry removal) of aerosol during long-range transport to the background marine sampling area [*Gogou et al.*, 1996]. In the forest aerosol, *n*-alkanes, rather, were associated (~82%, calculated from Table 5) with particles <1.5 μm. The CPI for all particle sizes was >2.0 (Table 5) and is reflected the predominant biogenic origin of the forest aerosol. UCM was associated mostly with particles <0.5 μm, while WNA were, rather, associated with particles >1.5 μm (Table 5). In order to reliably differentiate (between the three sampling sites) the *n*-alkanes particle size distribution, Lundgren diagrams [*Van Vaeck and Van Cauwenberghe*, 1985; *Aceves and Grimalt*, 1993] were constructed (Figure 1), and mass median aerodynamic diameters (MMAD) were

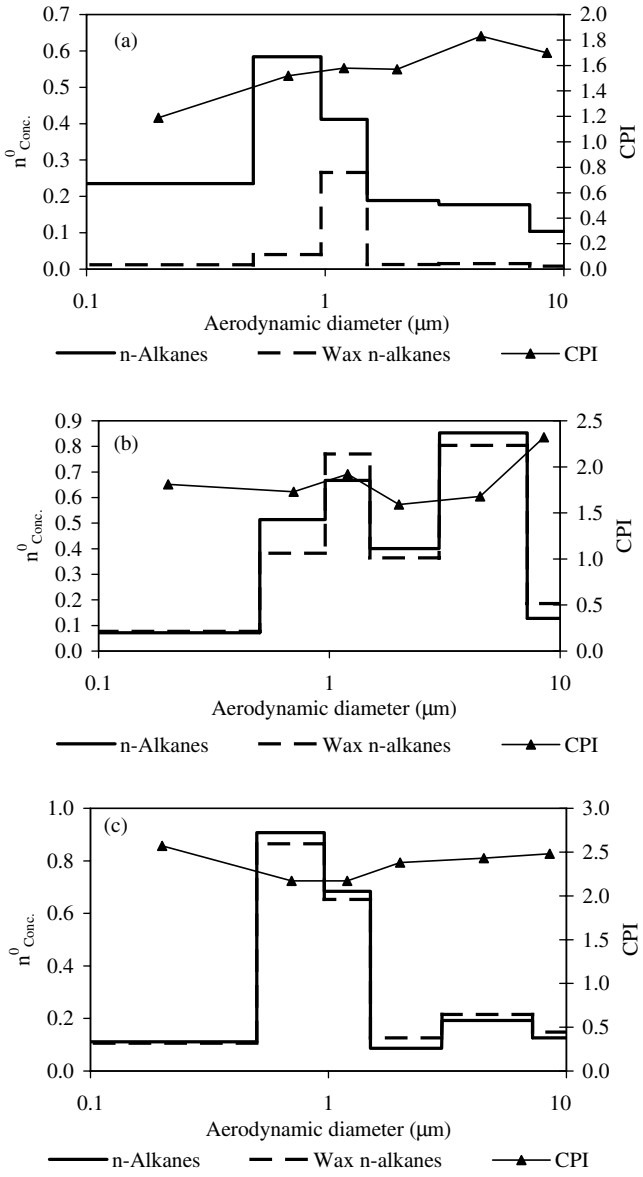

Figure 1. Lundgren diagrams for (a) urban, (b) background marine, and (c) forest *n*-alkanes, wax *n*-alkanes concentration, and carbon preference index (CPI).

calculated for total particle size range and also separately for fine (<2.5 μm) and coarse (>2.5 μm) particles (Table 6). For the coarse particles, *n*-alkanes MMAD did not differ greatly for the three aerosol types (Table 6 [see also *Aceves and Grimalt*, 1993]. Conversely, *n*-alkanes MMAD, for the total particle size range, was 0.45 μm for the urban aerosol and 2.00 μm and 0.63 μm for the background marine and forest aerosols, respectively (Table 6). The corresponding values for the fine particles were 0.38 μm for the urban site, 0.81 μm for the background marine, and 0.49 μm for the forest sites (Table 6). The above data indicate a clear differentiation between the background marine aerosol and the urban and forest aerosols. This difference in the MMAD (higher values for marine aerosol) can be interpreted by the particle-size changes of aerosol during long-range transport in the background marine area [see also *Van Vaeck and Van Cauwenberghe*, 1985]. The same effect can be observed when *n*-alkanes Lundgren diagrams are considered (Figure 1). The maxima of the distribution are shifted toward larger particle sizes for both total *n*-alkanes and wax *n*-alkanes in the marine background aerosol (Figure 1b) in comparison with

Table 6. Mass Median Aerodynamic Diameter (in μm) of Molecular Markers Calculated for the Whole Range of Impactor Particle Sizes (Total) and for Fine and Coarse Particles

	Urban			Marine			Forest		
	Total	Fine	Coarse	Total	Fine	Coarse	Total	Fine	Coarse
n-Alkanes	0.45 ± 0.02	0.38 ± 0.03	6.01 ± 0.04	2.00 ± 0.15	0.81 ± 0.01	5.78 ± 0.05	0.63 ± 0.04	0.49 0.01	6.60 0.04
PAHs	0.36 ± 0.03	0.34 ± 0.03	4.81 ± 0.06	0.73 ± 0.08	0.50 ± 0.03	7.20 ± 0.07	0.61 ± 0.05	0.50 0.02	7.20 0.03
n-Alkanals	0.44 ± 0.02	0.40 ± 0.05	3.47 ± 0.03	1.15 ± 0.08	1.00 ± 0.01	3.42 ± 0.06	ND	ND	ND
n-Alkanols	2.30 ± 0.12	0.70 ± 0.05	5.82 ± 0.01	2.69 ± 0.09	1.05 ± 0.03	4.47 ± 0.02	1.67 ± 0.11	0.96 ± 0.03	7.20 ± 0.05
n-Alkanoic acids	0.71 ± 0.05	0.71 ± 0.07	5.96 ± 0.02	0.62 ± 0.02	0.50 ± 0.00	4.73 ± 0.07	0.91 ± 0.06	0.62 ± 0.02	4.20 ± 0.04
n-Alkenoic acids	0.86 ± 0.04	0.80 ± 0.34	4.20 ± 0.02	1.65 ± 0.06	0.94 ± 0.01	5.36 ± 0.06	1.22 ± 0.08	0.76 ± 0.02	5.15 ± 0.02
α,ω-Dicarboxylic acids	0.34 ± 0.01	0.34 ± 0.02	5.96 ± 0.08	0.77 ± 0.04	0.77 ± 0.02	ND	0.34 ± 0.01	0.31 ± 0.01	3.55 ± 0.01
Pinonaldehyde	ND	ND	ND	ND	ND	ND	0.66 ± 0.03	0.66 ± 0.03	ND
Nopinone	ND	ND	ND	ND	ND	ND	0.30 ± 0.05	0.30 ± 0.05	ND
Pinonic acid	ND	ND	ND	ND	ND	ND	0.28 ± 0.02	0.28 ± 0.02	ND

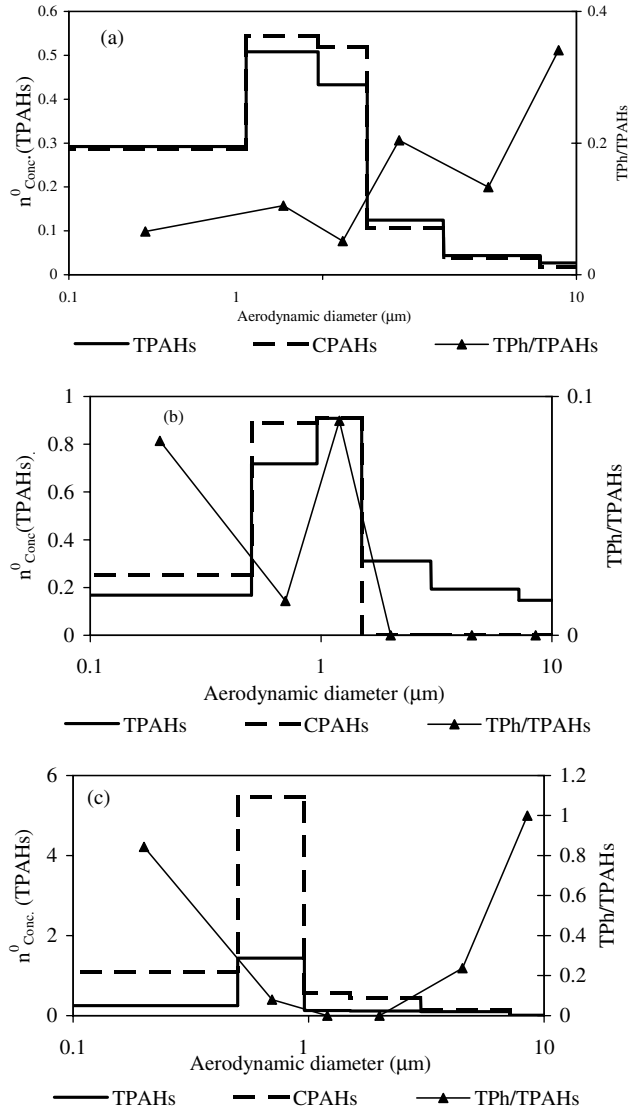

Figure 2. Lundgren diagrams for (a) urban, (b) background marine, and (c) forest total polynuclear aromatic hydrocarbons (TPAHs), combustion-derived PAHs (CPAHs), and total phenanthrenes (TPHs) concentration.

urban (Figure 1a) and forest aerosols (Figure 1c). Considering Lundgren diagrams for individual *n*-alkanes with different subcooled liquid vapor pressures (P_L^o), such as *n*-nonadecane (log P_L^o − 4.76 [*Pankow*, 1997]), *n*-nonadecane (log P_L^o − 6.87 [*Pankow*, 1997]), and *n*-hentriacontane, we also observed the same phenomenon as for total and wax *n*-alkanes: The maxima of the distribution were shifted toward larger particle sizes for the above homologues in the marine background aerosol. In urban aerosol a difference in particle size distribution was observed between total *n*-alkanes and wax *n*-alkanes (Figure 1a). The distribution maximum for the wax *n*-alkanes corresponds to larger particle sizes (>1 μm) than the corresponding for total *n*-alkanes (<1 μm) (Figure 1a). This observation is concomitant with the measured CPI values, which indicated a mixed origin for urban *n*-alkanes associated with particles >1 μm and a more petroliferous origin for the submicron particles (Figure 1a). In the marine aerosol the Lundgren diagrams (Figure 1b) demonstrate similar particle size distribution patterns for total *n*-alkanes and wax *n*-alkanes, as results of the mixing occurred during long-range transport to this site.

[15] Polynuclear aromatic hydrocarbons (PAHs) in the three different aerosol types exhibited a predominant occurrence in the particle size fraction <1.5 μm (93% for urban, 74% for marine, and 79% for the forest calculated from Tables 3, 4, and 5, respectively). In the urban aerosol, PAHs had a MMAD for the total particle size range of 0.36 μm (Table 6) and predominance in the fraction of particles <0.5 μm (∼70% as calculated from Table 3; Figure 2a). This observation indicates that PAHs size distribution basically reflects the gas-to-particle condensation in the submicron range after their emission to the urban atmosphere and subsequent cooling. This trend is more obvious if we consider the ratio of concentration of combustion-related PAHs (nine major nonalkylated compounds: fluoranthene, pyrene, benz[a]anthracene, chrysene, benzofluoranthenes, benzo[a]pyrene, benzo[e]pyrene, indeno[1,2,3-cd]pyrene, and benzo[ghi]perylene) (CPAHs) to the corresponding concentration of total PAHs (TPAHs) (CPAHs/TPAHs). The sum of parent PAHs expressed as CPAHs is used hereafter to represent pyrolytic PAH sources. The highest ratios are observed for particles <1.5 μm (0.67–0.82; Table 3). Conversely, the corresponding ratio of petrogenic PAHs (phenanthrene, methyl- and dimethyl-phenanthrene) (TPh) (TPh/TPAHs [*Gogou et al.*, 2000]) to the total PAHs reached their highest values in the urban atmosphere in particles >1.5 μm (0.14–0.34; Table 3). The size distributions were consistent with the condensation of large nonvolatile PAHs (e.g., compounds belonging to the CPAHs such as benzo[a]pyrene, benzo[e]pyrene, indeno[cd]pyrene, and benzo[ghi]perylene) (Figure 2a) on small particles during cooling of exhaust in the urban environment. The smaller, semivolatile PAHs (e.g., phenanthrene, methyl- and dimethyl-phenanthrene) expressed as TPh here represent the petrogenic PAH sources (unburned fossil fuels) in this study [*Gogou et al.*, 2000]. TPh became distributed between the smaller and larger particles (TPh/TPAHs in Tables 3 and 5 and Figures 1a and 1c), probably via continuing vaporization and condensation processes in the urban and forest atmospheres. *Venkataraman and Friedlander* [1994] made similar observations for polynuclear aromatic hydrocarbons in ambient aerosols. The MMAD calculated for PAHs associated with fine particles in the urban site was 0.34 μm (Table 6). This value was very similar to the corresponding one calculated for the total particles size range (0.36 μm; Table 6). The PAHs MMAD for the total particle size range was 0.73 μm for the marine aerosol and 0.63 μm for the forest aerosol (Table 6). The effect of particle size changes, due to transport, is reflected on both marine [*Gogou et al.*, 1996] and forest [*Kavouras et al.*, 1998b] aerosol for PAHs. *Van Vaeck and Van Cauwenberghe* [1985] have had similar observations in Belgium.

[16] The *n*-Alkanals were detected in all impactor stages for the urban and the background marine aerosol. No detectable amounts of these compounds could be detected in the impactor stages for forest aerosol (Tables 3–5). Considerable differences in aerosol composition and particle size distribution among *n*-alkanals were observed between urban and background marine areas. The *n*-Alkanals from C_9 to C_{23}, were detected in the urban site, maximizing at C_{17} and C_{22} (Table 3). Higher molecular weight *n*-alkanals from C_{18} to C_{28}, maximizing at C_{26} and C_{28}, were identified in background marine aerosol (Table 4). The occurrence of low molecular weight *n*-alkanals in the urban atmosphere can be explained by photooxidation reactions of anthropogenic hydrocarbons (such as alkenes) in urban areas [*Atkinson*, 1990]. Conversely, biogenic sources are on the origin of *n*-alkanals in the background marine atmosphere (Table 4 [see also *Stephanou*, 1989]). This is further supported by the strong even-to-odd predominance (CPI 2.0–8.1; Table 4). In urban aerosol, *n*-alkanals were primarily associated with ultrafine and fine particles (<0.96 μm; Table 3). The concentration levels of *n*-alkanals in all impactor stages were comparable (Table 3). The Lundgren diagram (Figure 3a) of *n*-alkanals, suggests a lognormal distribution as a function of particle size. The MMAD

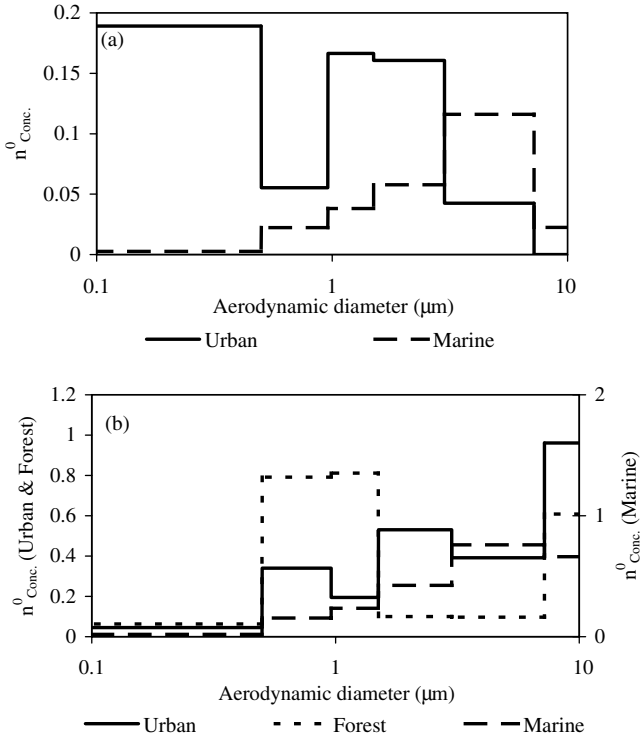

Figure 3. Lundgren diagrams for urban, background marine and forest (a) *n*-alkanals and (b) *n*-alkanols concentration.

calculated for *n*-alkanals for the total particle size range in the urban site was 0.44 μm (Table 6). The corresponding value for the marine aerosol MMAD was 1.15 μm (Table 6). The changes for marine aerosol due to transport were also reflected on *n*-alkanals MMAD. Thus the MMAD calculated for *n*-alkanals associated with fine particles in the urban site was 0.40 μm (Table 6). As for PAHs, this value was very similar to the corresponding value calculated for the total particles size range (0.44 μm; Table 6). The Lundgren size distribution pattern and the data of MMAD calculation indicate a strong effect of coagulation and agglomeration processes during *n*-alkanals residence in the urban atmosphere. The origin of *n*-alkanals in the marine aerosol has a more biogenic character, and this was reflected in their CPI (up to 6.2; Table 4) and high MMAD (1.00 μm for the fine particles; Table 6) values.

[17] The *n*-Alkanols were detected in all aerosol samples (Table 1). This compound class has mostly a biogenic origin, and therefore its composition and concentration levels in the three different aerosols did not differ greatly. The *n*-Alkanols ranging from C_{14} to C_{32}, with maxima at C_{26} and C_{28}, were detected in all particle sizes sampled in the urban area (Table 3). Their composition in background marine and forest aerosol samples was similar ($C_{12}-C_{20}$ with maxima at C_{24} and C_{28} for the marine aerosol and $C_{12}-C_{28}$ with maximum at C_{26} for the forest aerosol; Tables 4 and 5) to the composition of the urban ones. The high CPI values for all size fractions in urban (CPI 3.1–6.5; Table 3), background marine (CPI 2.9–11.1; Table 4), and forest aerosol (CPI >30.9; Table 5) strongly suggest direct emission from epicuticular waxes of higher terrestrial plants. The MMAD calculated for *n*-alkanols for the total particle size range in the urban site was 2.30 μm (Table 6). This value was the highest calculated among those for the other compound categories (Table 6). The corresponding MMAD for marine aerosol was 2.69 μm and 1.67 μm for the forest aerosol (Table 6). The effect of physical changes due to transport was reflected in a lower degree on marine aerosol for *n*-alkanols than for *n*-alkanals and *n*-alkanes (Table 6). Forest *n*-alkanols had a lower MMAD probably due to the vicinity of the emission source to the sampling site. The calculated MMAD for *n*-alkanols associated to fine particles was 0.70 μm in the urban site, 1.05 μm in the background marine site, and 0.96 μm in the forest site (Table 6). The comparison of MMAD of *n*-alkanols calculated for fine particles (Table 6) with the corresponding MMAD of *n*-alkanes, *n*-alkanals, and PAHs demonstrate the predominant biogenic character of *n*-alkanols in relation to the other compound classes. The *n*-alkanols particle size distribution patterns were further studied by using Lundgren diagrams (Figure 3b). A clear bimodal particle size distribution pattern was observed for forest *n*-alkanols (Figure 3b), while in the urban and marine aerosols, *n*-alkanols, rather, were associated with particles >1.5 μm.

[18] Minor differences in the composition of saturated acids were observed, as a function of particle size, among the three different aerosol types (Tables 3–5). The *n*-alcanoic acids ranged from C_8 to C_{30} (Tables 3–5). Palmitic acid (C_{16}) was the predominant compound in the carboxylic fraction of all analyzed samples. Low molecular weight acids such as octanoic (C_8) and nonanoic (C_9) acid were identified in the fine and ultrafine fractions (<1.5 μm)

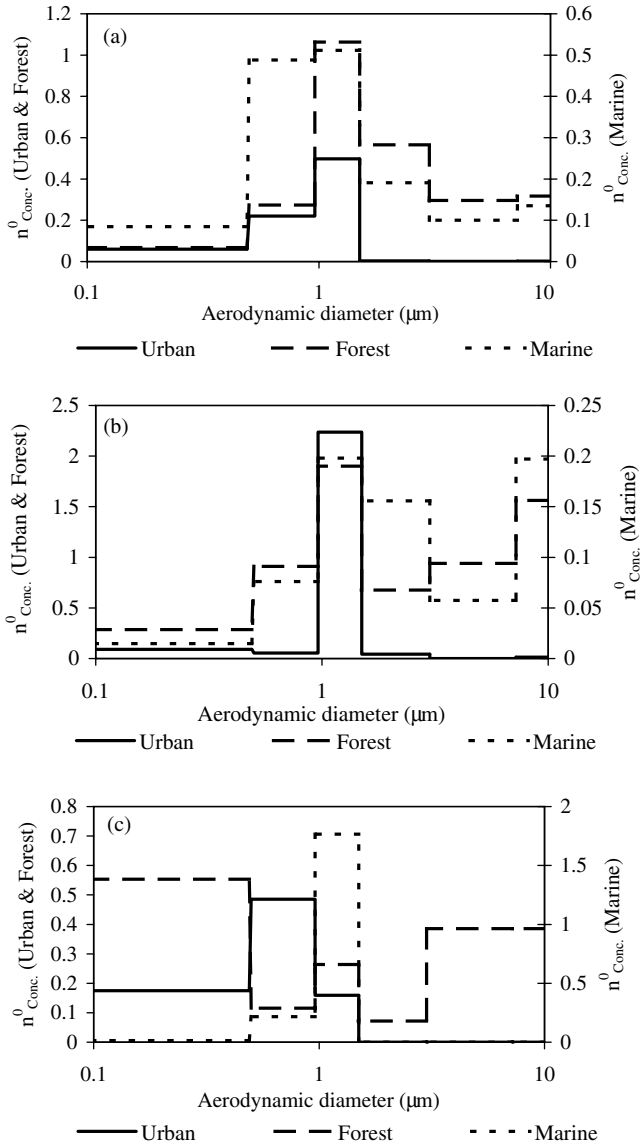

Figure 4. Lundgren diagrams for urban, background marine, and forest (a) *n*-alkanoic, (b) *n*-alkenoic, and (c) dicarboxylic acid concentration.

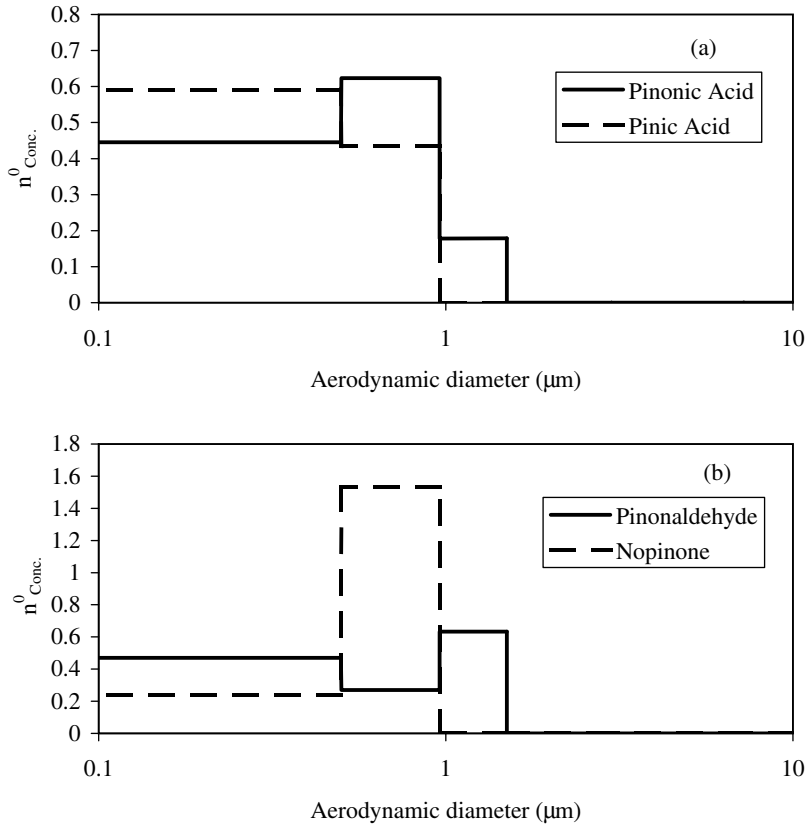

Figure 5. Lundgren diagrams for forest (a) carboxyl and (b) carbonyl photooxidation products of monoterpenes concentration.

of urban and background marine samples (Tables 3 and 4). Conversely, higher molecular weight carboxylic acids (>C_{24}) were mostly associated with particles >1.5 μm (Tables 3–5). Higher concentrations of *n*-alkanoic acids, associated with particles >1.5 μm, were measured in the forest atmosphere (from 9.9 to 44.0 ng m^{-3}; Table 5) than the other sites (urban, 0.2–0.9 ng m^{-3} (Table 3); background marine, 1.7–4.3 ng m^{-3} (Table 4)). The *n*-alkanoic acid concentration levels in fine and ultrafine fractions (<1.5 μm) were considerably higher for urban (Table 3) and forest (Table 5) aerosols. The enrichment of *n*-alkanoic acids at particles <1.5 μm was observed in the urban environment (Figure 4a and Table 3). This was also true for a large fraction of *n*-alcanoic acids in marine and forest aerosol (Figure 4a and Tables 4 and 5); however, a second maximum was also observed for larger particles (>7.2 μm).

[19] The strong even-to-odd predominance expressed by the high CPI values suggests that direct emission from epicuticular waxes of higher terrestrial plants was the predominant source in urban (CPI 10.6–19.1; Table 3), marine (CPI 11.1–24.5; Table 4), and forest (5.0–8.8; Table 5) aerosol. These results imply that biogenic organic acids may be associated with both fine and coarse particles. In general, *n*-alkanoic acids originate from a variety of sources, and therefore their specific origin reconciliation should be cautious [*Simoneit*, 1999; *Rogge et al.*, 1993a, 1993b, 1993c, 1993d, 1994].

[20] A series of monounsaturated (*n*-alkenoic) acids were detected in ambient samples. Palmitoleic ($C_{16:1}$) and oleic ($C_{18:1}$) acids were detected in all samples (Tables 3–5). Higher molecular weight unsaturated acids (up to $C_{20:1}$; Table 4) were detected in background marine aerosol. In addition, pentadecenoic acid ($C_{15:1}$) was identified in forest aerosol (Table 5). This variability can be explained by the contribution of other sources to marine aerosol such as phytoplankton [*Gogou et al.*, 1996]. The concentrations of *n*-alkenoic acids measured in all impactor stages in the marine area (from 0.3 to 1.0 ng m^{-3}; Table 4) were lower than those measured in urban (0.2–6.2 ng m^{-3}; Table 3) and forest (from 3.5 to 9.0 ng m^{-3}; Table 5) aerosol. High concentrations of *n*-alkenoic acids were associated with large particles in forest samples (e.g., >3.0 μm, 3.5–6.4 ng m^{-3}; Table 5). The particle size distribution pattern of *n*-alkenoic acids in the urban area suggests their association with particles <1.5 μm (Figure 4b). Conversely, the corresponding Lundgren diagram for marine and forest aerosol demonstrated a bimodal profile (Figure 4b). These differences suggest different sources for *n*-alkenoic acids among the sampling sites. Emissions of *n*-alkenoic acids from higher terrestrial plants in the forest were associated with large particles. Coagulation and agglomeration between particles along with local emissions of large particles may be the major source of *n*-alkenoic acids in the background marine area.

[21] The photooxidation products of unsaturated acids, α, ω-dicarboxylic acids, were detected in ambient sample in all sites (Tables 1 and 3–5). In all samples, α, ω-dicarboxylic acids ranged from C_6 to C_{15} (Tables 3–5). The homologue distribution maximized at azelaic (C_9) acid. The C_5 and C_6 homologues are formed by the oxidation of cyclic olefins [*Stephanou and Stratigakis*, 1993] and other emission sources [*Rogge et al.*, 1993a, 1993b, 1993c, 1994, 1998], while the C_8 and C_9 ones (the most abundant; see Tables 3–5) are formed by photooxidation of unsaturated carboxylic acids such as oleic ($C_{18:1}$) and linoleic ($C_{18:2}$) acids [*Stephanou*, 1992; *Stephanou and Stratigakis*, 1993]. Since oleic ($C_{18:1}$) and linoleic ($C_{18:2}$) acids are products of atmospheric reactions in both gas and particle phase [*Stephanou*, 1992; *Stephanou and Stratigakis*, 1993], they were mainly detected in the fine and ultrafine particles (<1.5 mm) in all areas (Figure 4c and Tables 3–5).

[22] Finally, series of carbonyl and carboxyl compounds were detected in forest samples. The chemical structure of these com-

pounds was identified by their mass spectra [*Kavouras et al.*, 1999b]. These compounds were pinonic acid, pinic acid, pinonaldehyde and nopinone, and are considered as photooxidation products of α- and β-pinene [*Kavouras et al.*, 1999a, 1999b]. It was recently proven that these compounds were responsible for the formation of secondary organic aerosol over forests [*Kavouras et al.*, 1998b, 1999a, 1999b]. As it is shown in Lundgren diagrams (Figure 5) both carbonyl and carboxyl compounds were primarily associated with particles <0.96 μm. More than 90% of pinonic and pinic acid and nopinone was associated with particles <0.96 μm (Table 5). A high amount of pinonaldehyde was associated with particles with a diameter from 0.5 to 0.96 μm. These results suggest these compounds may be responsible for the higher aerosol and organic extract mass in smaller particle sizes (Table 2).

[23] The comparison of MMAD, calculated for the total particle size range and for fine particles, between *n*-alkanoic (0.71, 0.62, and 0.91 μm; Table 6), *n*-alkenoic (0.86, 1.65, and 1.22 μm; Table 6), dicarboxylic acids (0.34, 0.77, 0.34 μm; Table 6), and monoterpene photooxidation products (0.28–0.66 μm; Table 6) reflects the processes of aerosol formation for these compound classes. A secondary process is responsible for the occurrence of dicarboxylic acids and monoterpene photooxidation products, while direct emission is responsible for the presence of *n*-alkanoic and *n*-alkenoic acids. However, our results indicate that the role of higher molecular weight carbonyl and carboxyl compounds might also be important for the formation of ultrafine particles in the atmosphere.

4. Conclusion

[24] The size distribution of organic aerosol in urban, marine background, and forest areas was characterized on the basis of MMAD calculation and Lundgren diagram construction. Most of the extractable organic (up to 85%) matter was associated in all cases with fine particles (<1.5 μm). Urban aerosol extractable organic mass was distributed between fine particles with a MMAD of 0.60 μm and coarse particles with a MMAD of 5.59 μm. For the forest aerosol, extractable organic mass was distributed between fine particles with MMAD of 0.36 μm and coarse particles with a MMAD of 5.13 μm. Organic molecular markers characterized in the three different aerosol types have shown that size distribution was primarily related to the emission source of these compounds. In addition, the effect of coagulation and nucleation might be significant in specific areas (e.g., urban environment). In particular, *n*-alkanes were mostly associated with fine particles in the urban and forest aerosols, and their total MMAD was 0.45 μm and 0.63 μm, respectively. In the background marine aerosol, *n*-alkanes were more evenly distributed, and their MMAD was 2.00 μm, showing physical changes due to long-range transport. Similar observations have been done for PAHs and *n*-alkanals. Conversely, the most biogenic compound class, namely *n*-alkanols, were evenly associated in the urban, background marine, and forest aerosols, between fine and coarse particles, and their corresponding total MMADs were 2.45, 2.69, and 1.67 μm, respectively. Saturated and unsaturated acids were mainly concentrated in the fine fraction; however, high concentrations of acids were detected in the coarse fraction of forests. The total MMADs of *n*-alkanoic acids were 0.71, 0.62, and 0.91 μm in the urban, background marine, and forest aerosols, respectively. Several low molecular weight organic compounds associated with photochemical reactions in the atmosphere were detected in urban marine and forests aerosols. Specifically, nonanal (urban), azelaic acid (urban and marine), pinonic acid, pinonaldehyde, pinic acid, and nopinone (forest) were found in the fine and ultrafine fraction showing the low total MMAD (0.28–0.77 μm) in the aerosol types studied.

[25] **Acknowledgments.** European Commission (DGXII, Environment and Climate Program, ENV4-CT95-0049) and the Special Research Account of the University of Crete are acknowledged for financial support. We thank N. Stratigakis and N. Mihalopoulos for their assistance during sampling.

References

Aboulkassim, T. A. T., and B. R. T. Simoneit, Lipid geochemistry of surficial sediments from the coastal environment of Egypt, 1, Aliphatic hydrocarbons-characterization and source, *Mar. Chem.*, *54*, 135–158, 1996.

Aceves, M., and J. O. Grimalt, Seasonally dependent size distributions of aliphatic and polynuclear hydrocarbons in urban aerosols from densely populated areas, *Environ. Sci. Technol.*, *27*, 2896–2908, 1993.

Allen, J. O., N. M. Dookeran, K. Taghizadeh, A. L. Lafleur, K. A. Smith, and A. F. Sarofim, Measurement of oxygenated polycyclic aromatic hydrocarbons associated with a size-segregated urban aerosol, *Environ. Sci. Technol.*, *31*, 2064–2070, 1997.

Andreae, M. O., R. W. Talbot, T. W. Andreae, and R. C. Harris, Formic and aceic acid over the central Amazon region, Brazil, 1, Dry season, *J. Geophys. Res.*, *92*, 6635–6641, 1988.

Ansari, A. S., and S. N. Pandis, Water absorption by secondary organic aerosol and its effect on inorganic aerosol behavior, *Environ. Sci. Technol.*, *34*, 71–77, 2000.

Atkinson, R., Gas-phase troposperic chemistry of organic compounds: A review, *Atmos. Environ.*, *24A*, 1–41, 1990.

Atkinson, R., and J. Arey, Atmospheric chemistry of biogenic organic compounds, *Account. Chem. Res.*, *31*, 574–583, 1998.

Chow, J. C., J. G. Watson, D. H. Lowenthal, P. A. Solomon, K. L. Magliano, S. D. Ziman, and L. W. Richards, PM_{10} and $PM_{2.5}$ compositions in California's San Joaquin Valley, *Aerosol Sci. Technol.*, *18*, 105–128, 1993.

Chow, J. C., J. G. Watson, E. M. Fujita, Z. Q. Lu, D. R. Lawson, and L. L. Ashbaugh, Temporal and spatial variations of $PM_{2.5}$ and PM_{10} aerosol in the Southern California Air Quality Study, *Atmos. Environ.*, *28*, 2061–2080, 1994.

Cruz, C. N., and S. N. Pandis, The effect of organic coatings on the cloud condensation nuclei activation of inorganic atmospheric aerosol, *J. Geophys. Res.*, *103*, 13,111–13,123, 1998.

Fernandes, M. B., M. A. Sicre, I. Broyelle, A. Lorre, and D. Pont, Contamination by polycyclic aromatic hydrocarbons (PAHs) in French and European rivers, *Hydrobiologia*, *410*, 343–348, 1999.

Gogou, A., N. Stratigakis, M. Kanakidou, and E. G. Stephanou, Organic aerosols in Eastern Mediterranean: Components source reconciliation by using molecular markers and atmospheric back trajectories, *Org. Geochem.*, *25*, 79–96, 1996.

Gogou, A., M. Apostolaki, and E. G. Stephanou, Determination of organic molecular markers in marine aerosols and sediments: One-step flash chromatography compounds class fractionation and capillary gas chromatographic analysis, *J. Chromatogr. A*, *799*, 215–231, 1998.

Gogou, A., I. Bouloubassi, and E. G. Stephanou, Marine organic geochemistry of the Eastern Mediterranean, 1, Aliphatic and polyaromatic hydrocarbons in Cretan Sea surficial sediments, *Mar. Chem.*, *68*, 265–282, 2000.

Hahn, J., Organic constituents of natural aerosol, *Ann. N. Y. Acad. Sci.*, *338*, 359–376, 1980.

Jaenicke, R., The role of organic material in atmospheric aerosols, *Pure Appl. Geophys.*, *116*, 283–292, 1978.

Kavouras, I. G., N. Stratigakis, and E. G. Stephanou, Iso- and anteiso-alkanes: Specific tracers of environmental tobacco smoke in indoor and outdoor particle-size distributed urban aerosols, *Environ. Sci. Technol.*, *10*, 1369–1377, 1998a.

Kavouras, I. G., N. Mihalopoulos, and E. G. Stephanou, Formation of atmospheric particles from organic acids produced by forests, *Nature*, *395*, 683–686, 1998b.

Kavouras, I. G., N. Mihalopoulos, and E. G. Stephanou, Secondary organic aerosol formation vs. primary organic aerosol emission: In situ evidence for the chemical coupling between monoterpene acidic photooxidation products and new particle formation over forests, *Environ. Sci. Technol.*, *33*, 1028–1037, 1999a.

Kavouras, I. G., N. Mihalopoulos, and E. G. Stephanou, Formation and gas/particle partitioning of monoterpenes photo-oxidation products over forests, *Geophys. Res. Lett.*, *26*, 55–58, 1999b.

Lowenthal, D. H., B. Zielinska, J. C. Chow, J. G. Watson, M. Gautam, D. H. Ferguson, G. R. Neuroth, and K. D. Stevens, Characterization of heavy duty diesel vehicle emissions, *Atmos. Environ.*, *28*, 731–743, 1994.

Mihalopoulos, N., E. G. Stephanou, M. Kanakidou, S. Pilitsidis, and P. Bousquet, Tropospheric aerosol composition in the Eastern Mediterranean region, *Tellus, Ser. B*, *49*, 314–326, 1997.

Pagano, P., T. Zalamaco, E. Scarcella, S. Bruni, and M. Calamosca, Mutagenic activity of total particle-sized fractions of urban particulate matter, *Environ. Sci. Technol.*, *30*, 3512–3516, 1996.

Pandis, S. N., R. A. Harley, G. R. Cass, and J. H. Seinfeld, Secondary organic aerosol formation and transport, *Atmos. Environ.*, *26*, 2269–2282, 1992.

Pankow, J. F., Partitioning of semi-volatile organic compounds to the air/water interface, *Atmos. Environ.*, *31*, 927–929, 1997.

Rogge, W. F., L. Hildemann, M. A. Mazurek, G. R. Cass, and B. R. T. Simoneit, Sources of fine organic aerosol, 2, Noncatalyst and catalyst-equipped automobiles and heavy duty diesel trucks, *Environ. Sci. and Technol.*, *27*, 636–651, 1993a.

Rogge, W. F., L. Hildemann, M. A. Mazurek, G. R. Cass, and B. R. T. Simoneit, Sources of fine organic aerosol, 3, Road dust, tire debris and organometallic brake lining dust: Roads as sources and sinks, *Environ. Sci. Technol.*, *27*, 1892–1904, 1993b.

Rogge, W. F., L. Hildemann, M. A. Mazurek, G. R. Cass, and B. R. T. Simoneit, Sources of fine organic aerosol, 4, Particulate abrasion products from leaf surfaces of urban plants, *Environ. Sci. Technol.*, *27*, 2700–2711, 1993c.

Rogge, W. F., L. Hildemann, M. A. Mazurek, G. R. Cass, and B. R. T. Simoneit, Sources of fine organic aerosol, 5, Natural gas home appliances, *Environ. Sci. Technol.*, *27*, 2736–2744, 1993d.

Rogge, W. F., L. Hildemann, M. A. Mazurek, G. R. Cass, and B. R. T. Simoneit, Sources of fine organic aerosol, 6, Cigarette smoke in the urban atmosphere, *Environ. Sci. Technol.*, *28*, 1375–1388, 1994.

Rogge, W. F., L. Hildemann, M. A. Mazurek, G. R. Cass, and B. R. T. Simoneit, Sources of fine organic aerosol, 7, Hot asphalt roofing tar pot fumes, *Environ. Sci. Technol.*, *31*, 2726–2730, 1997a.

Rogge, W. F., L. Hildemann, M. A. Mazurek, G. R. Cass, and B. R. T. Simoneit, Sources of fine organic aerosol, 8, Boilers burning distillate fuel oil, *Environ. Sci. Technol.*, *31*, 2731–2737, 1997b.

Rogge, W. F., L. Hildemann, M. A. Mazurek, G. R. Cass, and B. R. T. Simoneit, Sources of fine organic aerosol, 9, Pine, oak and synthetic log combustion in residential fireplaces, *Environ. Sci. Technol.*, *32*, 13–22, 1998.

Russell, L. M., S. N. Pandis, and J. H. Seinfeld, Aerosol production and growth in the marine boundary layer, *J. Geophys. Res.*, *99*, 20,989–21,003, 1994.

Sicre, M. A., J. C. Marty, A. Saliot, X. Aparicio, J. Grimalt, and J. Albaiges, Aliphatic and aromatic hydrocarbons in different sized aerosols over the Mediterranean Sea: Occurrence and origin, *Atmos. Environ.*, *21*, 2247–2259, 1987.

Sicre, M. A., J. C. Marty, A. Lorre, and A. Saliot, Airborne and vapor-phase hydrocarbons over the Mediterranean Sea, *Geophys. Res. Lett.*, *17*, 2161–2164, 1990a.

Sicre, M. A., J. C. Marty, and A. Saliot, *n*-Alkanes, fatty acid esters and fatty acid salts in size fractionated aerosol collected over the Mediterranean Sea, *J. Geophys. Res.*, *95*, 3649–3657, 1990b.

Simoneit, B. R. T., A review of biomarker compounds as source indicators and tracers of air pollution, *Environ. Sci. Pollut.*, *6*, 159–169, 1999.

Stephanou, E. G., Long chain *n*-aldehydes: An ubiquitous compound class of environmental and geochemical significance, *Naturwissenschaften*, *76*, 464–467, 1989.

Stephanou, E. G., α, ω-Dicarboxylic acid salts and α, ω-dicarboxylic acids: Photo-oxidation products of unsaturated fatty acids, present in marine aerosols and marine sediments, *Naturwissenschaften*, *79*, 128–131, 1992.

Stephanou, E. G., and N. Stratigakis, Oxocarboxylic and α, ω-dicarboxylic acids: Photooxidation products of biogenic unsaturated fatty acids present in urban aerosols, *Environ. Sci. Technol.*, *27*, 1403–1407, 1993.

Talbot, R. W., A. S. Vijgen, and R. C. Harriss, Soluble species in the Arctic summer troposphere: Acidic gases, aerosol and precipitation, *J. Geophys. Res.*, *97*, 16,531–16,543, 1992.

Tao, Y., and P. H. McMurry, Vapor pressure and surface free energies of C_{14}–C_{18} monocarboxylic acids and C_5 and C_6 dicarboxylic acids, *Environ. Sci. Technol.*, *23*, 1519–1523, 1989.

Turpin, B. J., P. Saxena, and E. Andrews, Measuring and simulating particulate organics in the atmosphere: Problems and prospects, *Atmos. Environ.*, *34*, 2983–3013, 2000.

Van Vaeck, L., and K. Van Cauwenberghe, Characteristic parameters of particle size distributions of primary organic constituents of ambient aerosols, *Environ. Sci. Technol.*, *19*, 707–716, 1985.

Venkataraman, C., and S. K. Friedlander, Size-distribution of polycyclic aromatic hydrocarbons and elemental carbon, 2, Ambient measurements and effects of atmospheric processes, *Environ. Sci. Technol.*, *28*, 563–572, 1994.

I. G. Kavouras and E. G. Stephanou, Environmental Chemical Processes Laboratory, Department of Chemistry, University of Crete, GR-71409 Heraklion, Hellas, Greece. (stephanou@chemistry.uoc.gr)